Supplementary Information (SI) to accompany

Controlling self-assembly of microtubule spools via kinesin motor density

Amy T. Lam, Corina Curschellas, Deepthi Krovvidi, and Henry Hess*

*Henry Hess

Columbia University

Department of Biomedical Engineering

351L Engineering Terrace

MC8904

1210 Amsterdam Avenue

New York, NY 10027

Fax: (212) 854-8725

Tel: (212) 854-7749

E-mail: hh2374@columbia.edu

This supplementary information contains three parts:

(1) Landing rate experiments

(2) Experiments with GFP-kinesin

(3) Sample images for each section at each time point for experiments described in the main text

(4) Analysis of spool brightness

(1) Landing rate experiments

It is possible to estimate the kinesin density by performing a landing rate experiment.[1] In these experiments, the kinesin gradient is created as described in the main text. Then a solution containing fluorescently labeled microtubules and antifade is flowed into the flow cell. Rather than using ATP, the non-hydrolyzable analogue, AMP-PNP, is used. The microtubules are sheared by passing the microtubule containing solution through a 30G1 needle (inner diameter ~0.159 mm) five times to shorten them. The edges of the flow cell are sealed with grease to prevent evaporation, and each section of the flow cell is imaged at regular intervals over the course of 20 minutes. The number of microtubules in the field of view is counted, and the landing rate of the microtubules is obtained by fitting the equation $N = N_{max}\left(1 - e^{-R(t - t_i)/N_{max}}\right)$ to the data (Supplementary Figure 1). Here, N is the number of microtubules landed, R is the landing rate, t is time, and t_i is the time of initial introduction of microtubules into the flow cell. R and t_i are fit parameters. This is then compared to the landing rates of known dilutions of kinesin, and thus the landing rate is used as an estimator for the kinesin density on the surface.

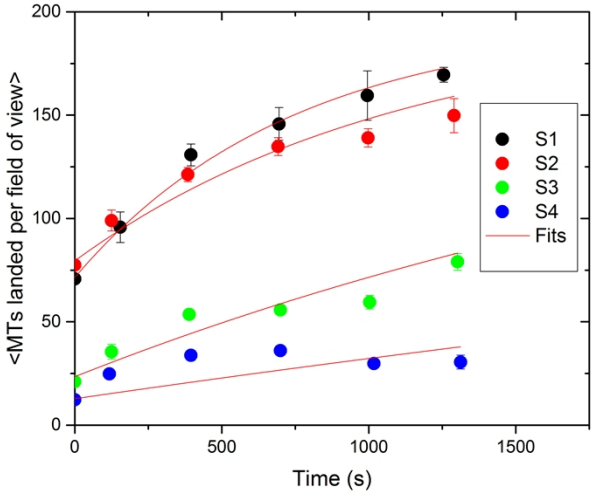

Supplementary Figure 1. The number of microtubules landed in each section versus time. The equation $N = N_{max}\left(1 - e^{-R(t-t_i)/N_{max}}\right)$ is fitted to the data. The landing rates for each section are used to estimate the relative kinesin densities.

The landing rate of the known dilutions of kinesin is also determined by fitting. The landing rates are then plotted as a function of the dilution factor, *d*, and the equation $R = Z(1 - e^{-Ad})$ is fit to the data, where *Z* and *A* are fit parameters. Using the values obtained by the fit, it is then possible to solve for the dilution factor and determine the relative densities of kinesin for each section. Using this method, we find that the densities of Sections II, III, and IV relative to Section I were found to be 0.55 ± 0.09, 0.17 ± 0.03, and 0.05 ± 0.02, respectively (Supplementary Table 1).

Supplementary Table 1. Fit parameters obtained from experimental data.

Parameter	Value	SEM
Z ($mm^{-2}\ s^{-1}$)	259.2	0.1
A (unitless)	28	5
R_{S1} ($mm^{-2}\ s^{-1}$)	160	10
R_{S2} ($mm^{-2}\ s^{-1}$)	110	10
R_{S3} ($mm^{-2}\ s^{-1}$)	40	7
R_{S4} ($mm^{-2}\ s^{-1}$)	14	5

Taking the ratio of the kinesin densities of the second, third, and fourth sections to the first section is given by

$$R = \frac{1}{4}(1 - f)^{S-1}(5 - S)$$

where f is the fraction of kinesin adsorbed per 2 minutes, and S is the section number, we can calculate that $f = 0.36 \pm 0.05$, i.e. $36 \pm 5\%$ of the kinesin adsorbs to the surface over 2 minutes. This adsorption rate is somewhat lower than the diffusion-limited adsorption rate of 50% per minute estimated for a kinesin diffusion constant of 20 $\mu m^2\ s^{-1}$ and a flow cell height of 100 μm.[2]

References:

1. A. Agarwal, E. Luria, X. P. Deng, J. Lahann and H. Hess, *Cellular and Molecular Bioengineering* 2012, **5**, 320-326.
2. J. Howard, A. J. Hunt and S. Baek, *Methods Cell Biol*, 1993, **39**, 137-147.

(2) Experiments with GFP-kinesin

Using GFP-kinesin allows us to image the kinesin motors enabling direct measurement of the kinesin density. However, because the GFP-kinesin must be attached to the surface through an antibody to support motility, it is likely that the spooling mechanics are affected as discussed below. Nevertheless, we created a gradient of GFP-kinesin motors and ran a similar experiment with biotinylated microtubules cross-linked via streptavidin, verifying that spooling is affected by kinesin density. The data from these experiments are presented here for completeness.

For these experiments, we used a kinesin construct containing the first 430 amino acids of kinesin-1 fused to an eGFP and a polyhistidine tag at the tail domain (rkin430eGFP), which was expressed in Escherichia coli and purified using a Ni-NTA column. Single molecule imaging of the GFP-kinesin was achieved by using an objective-type TIRF setup on an Eclipse Ti microscope (Nikon Instruments, Melville, NY) with a 100x/1.49 NA objective lens (Nikon Instruments, Melville, NY) using a 488 nm laser (maximum intensity 50 mW). To determine the kinesin density in each section, images of 3 different fields of view per section were taken using an iXon DU897 Ultra EMCCD Camera (Andor Technology, South Windsor, CT) with an exposure time of 0.2s. Imaging of the microtubules was achieved using an epifluorescence microscope (Nikon TE2000) equipped with an X-cite 120 lamp (EXFO, Ontario, Canada) and an iXON DU885LC EMCCD camera (Andor Technology, South Windsor, CT).

In our experience, the truncated GFP-kinesin does not support smooth motility of microtubules without the use of an antibody. Thus, instead of a kinesin gradient, we created a gradient of antibody by flowing the antibody solution in stepwise, pausing 40s between each step. After creating the antibody gradient, a solution of GFP-kinesin was flowed in. For single molecule imaging of the GFP-kinesin, the kinesin solution was diluted 100-fold further than for

the spooling assays. This allowed us to quantify the kinesin density for these experiments by counting well-separated fluorescent molecules (1.9 ± 0.3 μm^{-2}, 1.4 ± 0.2 μm^{-2}, and 1.2 ± 0.2 μm^{-2} for Sections I, II, and III, respectively) and thus estimate the kinesin density of the GFP-kinesin spooling assays. The excess kinesin was washed out with antifade, and then the GFP-kinesin was imaged using TIRF microscopy. For the spooling assays, after washing the excess kinesin out with antifade, the rest of the solutions were flowed in following the same protocol as in the main text.

The average spool densities for Sections I and II were 125 ± 5 mm^{-2} and 59 ± 1 mm^{-2}, respectively. The average spool circumferences for Sections I and II were 20 ± 2 μm and 26 ± 3 μm. No spools were observed in Section III (Supplementary Figure 2). The microtubules do not seem to be tethered as strongly to the surface, likely because the kinesin motors are also not as strongly attached to the surface. This would be a possible explanation for why fewer spools were observed as compared to the experiments done with conventional kinesin. Furthermore, during experiments, spools were observed to detach from the surface and diffuse. Thus, the spools observed in each section at the end of the experiment may not have originated from that section. However, the diffusion coefficient of these spools is expected to be much lower than that of single microtubules. This would explain why we still observe a larger number of spools of smaller circumference in the section with the highest kinesin density, lower spool density and larger spools in the section with an intermediate kinesin density, and no spools in the section with the lowest kinesin density (Supplementary Figure 2).

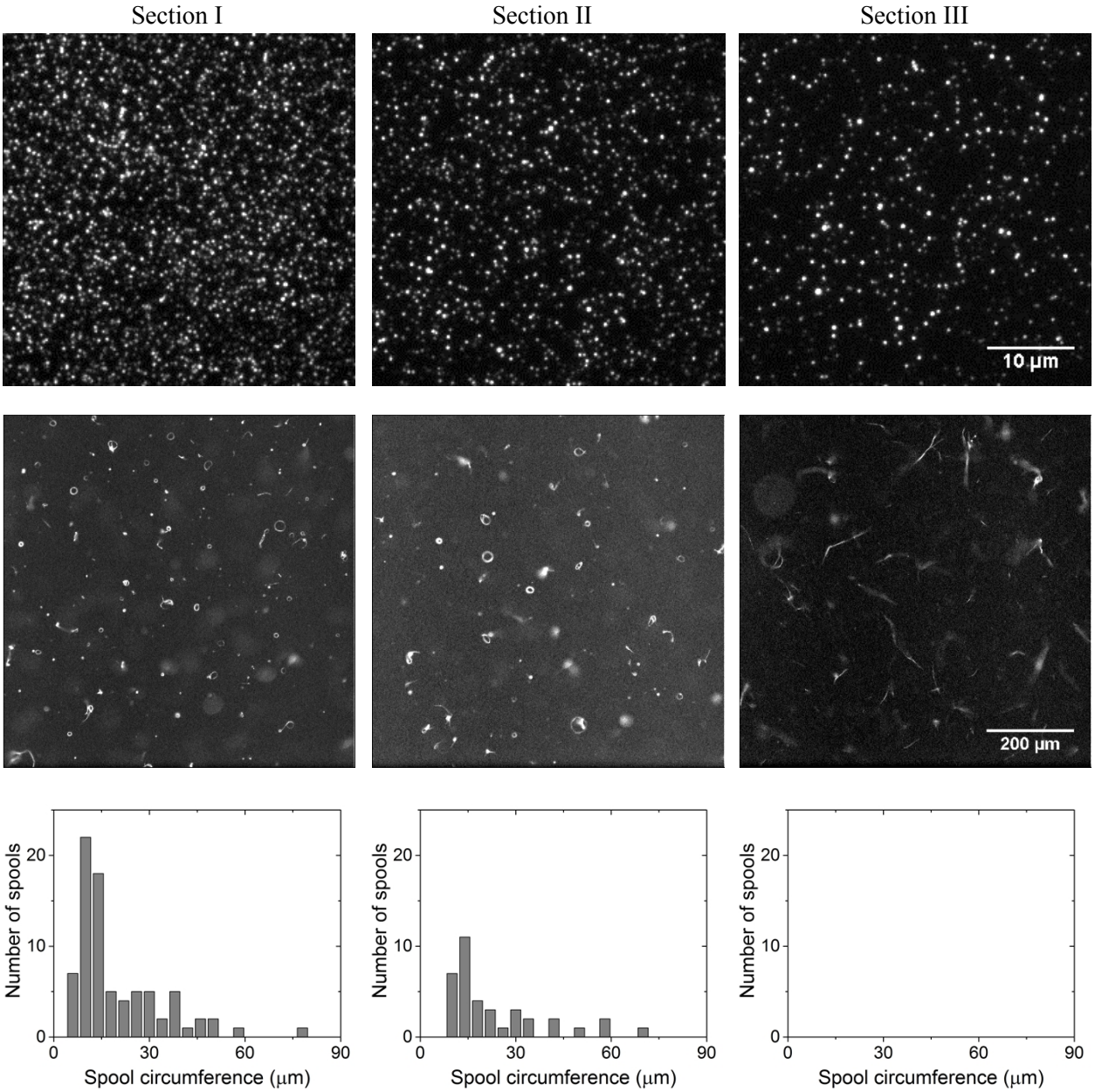

Supplementary Figure 2. The GFP-kinesin gradient and the resulting spool formation after 2 hours. Images of the GFP-kinesin were taken with TIRF microscopy with an 100x oil objective. Images of the spools were taken at 10x magnification using epifluorescence microscopy. The gradient of GFP-kinesin was created by first creating a stepwise gradient of anti-GFP antibodies to which the truncated GFP-kinesin adsorbed. The antibody was allowed to adsorb for 40s between each section, which resulted in kinesin densities of densities of 0.73 ± 0.04 and 0.64 ± 0.02 relative to Section I for Sections II and III, respectively. The resulting average spool densities for Sections I and II were 125 ± 5 mm^{-2} and 59 ± 1 mm^{-2}, respectively. The average spool circumferences for Sections I and II were 20 ± 2 µm and 26 ± 3 µm. No spools were observed in Section III. For single molecule imaging, the GFP-kinesin solution used was 100 times more dilute than the solution used for the spooling assays.

(3) Sample images for each section at each time point for experiments described in the main text:

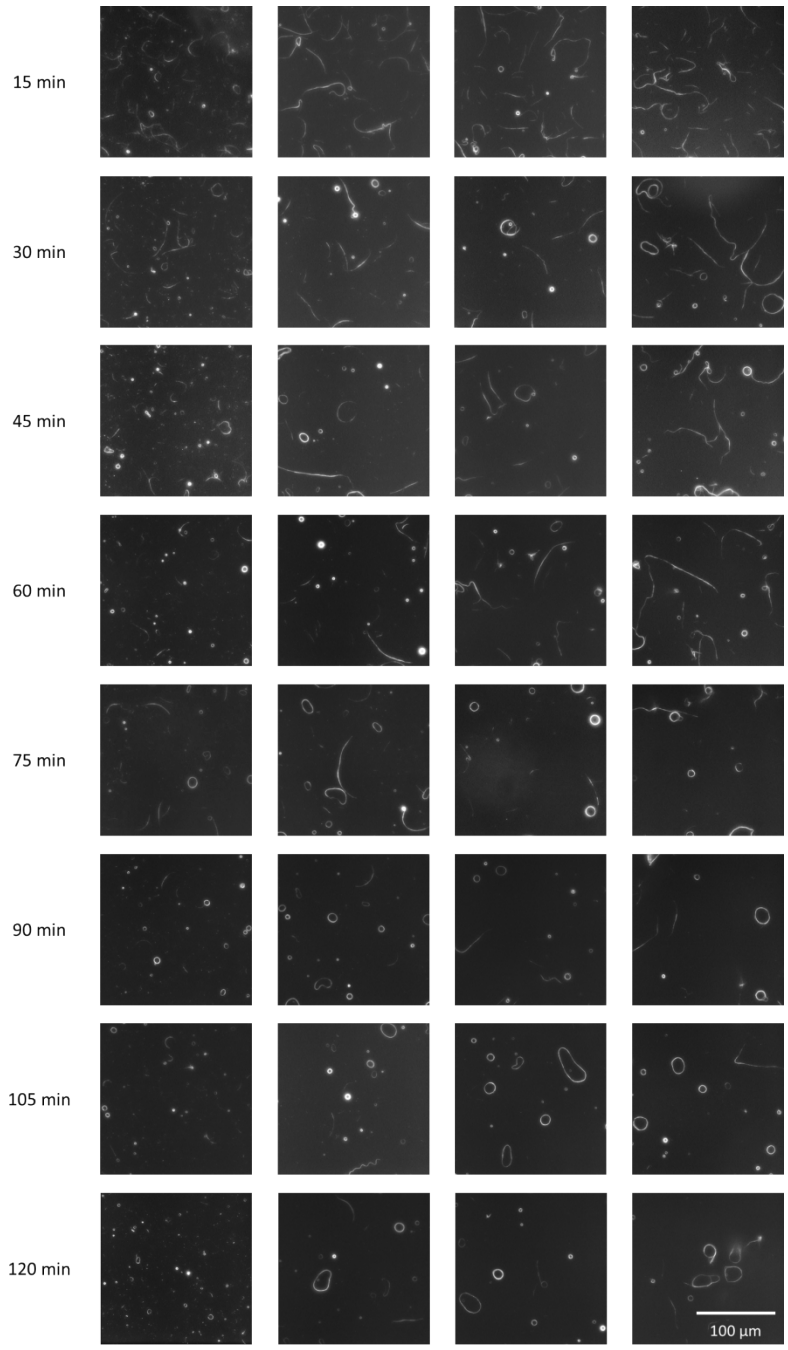

Supplementary Figure 3. Images from each section of the flow cell taken every 15 minutes. Section 1 has the highest density of kinesin while section 4 has the lowest. The initial microtubule densities for each section are roughly equal. Assembly reaches equilibrium at around 90 min for each section.

(4) Analysis of spool brightness

For each section, ten spools were chosen at random to be analyzed for brightness. At intervals of 45 degrees, the integrated intensity over the inner to outer diameter of the spool was measured. After subtracting the background, the average integrated intensity was normalized by the integrated intensity over the width of a single microtubule (240 ± 46 nm) to find the average number of microtubules per spool. The combined average of the number of microtubules making up spools for all sections is 11 ± 3, which is not significantly different from the sectional averages.

The spools were not necessarily consistent in brightness around the circumference, and on average had a difference of 6-9 microtubules between the brightest and least bright segments. The brightness of the spools is not obviously correlated with the circumference (Supplementary Figure 4).

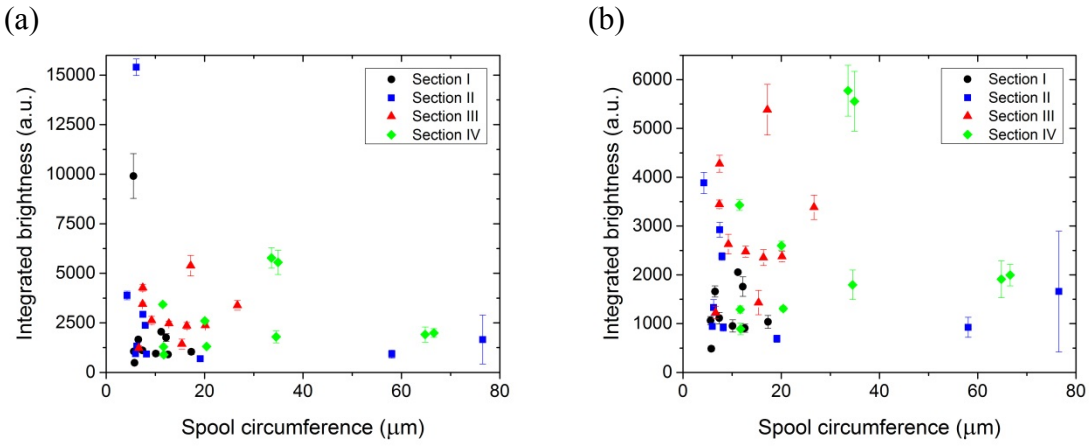

Supplementary Figure 4. The integrated brightness over the width of the spools does not obviously correlate with the spool circumference. Graph (a) contains the full data set and graph (b) is of the data set with outliers discarded.

The product of the average number of microtubules in a spool, average spool density, and average spool circumference can be used to estimate the total length of microtubules which spool

in each section. This was not found to be significantly different between sections using a one-way ANOVA test (Supplementary Table 2, Supplementary Figure 5).

Supplementary Table 2. The approximate length of microtubules taken up by spooling was calculated by taking the product of the average number of microtubules making the annular width of the spool, the average spool density, and the average spool circumference.

	Section 1	Section 2	Section 3	Section 4
Average spool brightness (a.u.)	2094 ± 881	3106 ± 1405	2898 ± 400	2655 ± 551
Average number of MTs making up spool width	8.7 ± 4.0	12.9 ± 6.4	12.1 ± 2.9	11.1 ± 3.1
Average spool density (mm^{-2})	610 ± 60	540 ± 40	280 ± 90	200 ± 40
Average spool circumference (μm)	7.9 ± 0.3	14.7 ± 1.4	18.3 ± 2.1	21.2 ± 2.3
Estimated microtubules in spools per unit area (mm/mm^{-2})	42 ± 20	103 ± 52	62 ± 26	47 ± 17

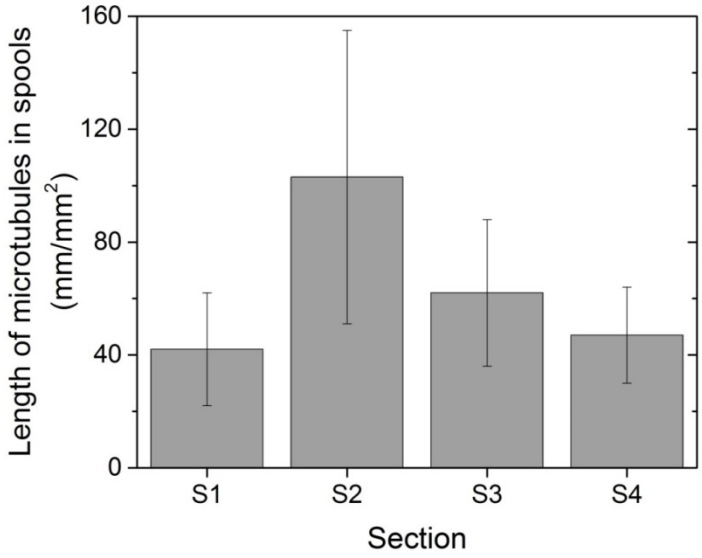

Supplementary Figure 5. The product of the average spool circumference, average spool density, and average number of microtubules per spool for each section provides a measure for the quantity of microtubules which have been taken up by spools. These values are not significantly different between sections by a one-way ANOVA ($F(3, 37) = 0.24$). Error bars represent the SEM.